# External intermittency compensation of dissipation scale distributions in a turbulent boundary layer

Sabah F. H. Alhamdi[1,2] and Sean C. C. Bailey[1,*]

[1]*Department of Mechanical Engineering, University of Kentucky, Lexington, Kentucky 40506, USA*

[2]*University of Misan, Amarah, Misan 62001, Iraq*

(Received 14 March 2018; published 10 July 2018)

The influence of external intermittency on the scaling of the dissipation scale distribution is examined in turbulent boundary layer flow at $\mathrm{Re}_\tau \approx 1000$. Probability density functions (PDFs) of the dissipative scales are compared with, and without, accounting for the external intermittency using an intermittency detection function. Results showed that accounting for the external intermittency produces better consistency in the shapes of the PDFs at the same wall-normal location at different instances in time. In addition, properly scaling the dissipation scale distribution collapses the probability density functions calculated at different wall-normal locations. This improvement in the scaling of the dissipation scale distribution supports prior observations of universality of the small-scale description of the turbulence for wall-bounded flow.

DOI: 10.1103/PhysRevFluids.3.074601

## I. INTRODUCTION

According to Kolmogorov's second hypothesis, an inertial subrange will form when the magnitude of the spatial separation vector $|\boldsymbol{r}|$ is much smaller than the scale $L$ at which kinetic energy is produced and much larger than the scale at which it is dissipated, described by the Kolmogorov scale $\eta_K$. Typically, $L$ is described using the longitudinal integral length scale which, for isotropic turbulence, can be found at a particular time, $t$, using the autocovariance

$$R_{ij}(\boldsymbol{r},\boldsymbol{x},t) = \langle u_i(\boldsymbol{x},t)u_j(\boldsymbol{r}+\boldsymbol{x},t)\rangle, \tag{1}$$

where $\boldsymbol{x} = x_i\hat{e}_i$ describes spatial location, with $\hat{e}_i$ the Cartesian basis vector in the $i$ direction, and $\boldsymbol{r} = r_i\hat{e}_i$ a spatial displacement. The fluctuating velocity vector $\boldsymbol{u} = u_i\hat{e}_i$ is found from the instantaneous velocity vector $\boldsymbol{U}$ through $\boldsymbol{u}(\boldsymbol{x},t) = \boldsymbol{U}(\boldsymbol{x},t) - \langle \boldsymbol{U}(\boldsymbol{x},t)\rangle$, where $\langle\,\rangle$ denotes an ensemble-averaged quantity. Finally, the longitudinal integral length scale at a particular location and time $L(\boldsymbol{x},t)$ is found from

$$L(\boldsymbol{x},t) = \frac{1}{\langle u_1(\boldsymbol{x},t)^2\rangle}\int_0^\infty R_{11}(r_1,\boldsymbol{x},t)dr_1, \tag{2}$$

where, in isotropic turbulence, the $x_1$ coordinate direction is arbitrary.

Within the inertial subrange the longitudinal structure function of order $n$,

$$S_n = \langle(\delta_r u)^n\rangle, \tag{3}$$

where

$$\delta_r u = (u_1(\boldsymbol{x}+r_1) - u_1(\boldsymbol{x})), \tag{4}$$

*sean.bailey@uky.edu

 

depends only on the mean rate of dissipation of turbulent kinetic energy, $\langle\varepsilon\rangle$. Within the inertial subrange the longitudinal structure function follows power law scaling such that

$$S_n = A_n \left( \frac{|\boldsymbol{r}|}{L} \right)^{\zeta_n}, \tag{5}$$

where $A_n$ are universal constants. Kolmogorov's theory predicted that $\zeta_n = n/3$. However, experimental investigations (e.g., Anselmet *et al.* [1]) have shown that the set of $\zeta_n$ differs from this linear scaling and has nonlinear dependence on $n$. This deviation from the expected behavior has been attributed to spatial intermittency in the fine structure of the turbulent flow (for example, see Frisch [2]). In other words, the dissipation does not occur homogeneously in space but is instead occurring in compact regions in space, separated by regions of little to no dissipation. This intermittency persists throughout the universal equilibrium range and, as a result, the use of a singular mean dissipation length scale to describe the turbulent dynamics does not appear to be sufficient [3].

In this context, an alternative description of the dissipation scale that incorporates the existence of an entire continuum of local dissipation scales becomes attractive. Previous researchers [4–6] have introduced the concept of a random field of dissipative scales, $\eta$. Effectively this scale can be found from instances $|\boldsymbol{r}| = \eta$ where the local Reynolds number $\mathrm{Re}_\eta = |\delta_r u| r_1/\nu \sim 1$. As such, the probability density function (PDF) of $\eta$ becomes an important defining characteristic. Yakhot [7] presented an analytical description of this PDF, which compared favorably to PDFs extracted direct numerical simulation (DNS) data of homogeneous isotropic turbulence [8] and at the centerline and outer region of pipe flow [9]. A closer look at the wall dependence of the PDFs conducted by Hamlington *et al.* [10] using DNS of channel flow indicated that, far away from the wall, the PDFs scaled with $\eta_0 = L\mathrm{Re}_L^{-0.73}$ and were in agreement with those observed by Schumacher [8] and Bailey *et al.* [9] where $\mathrm{Re}_L = \delta_L L/\nu$ with $\delta_L$ defined by Eq. (4) when $r_1 = L$. However, the PDFs near the wall no longer scaled by $\eta_0$. These results were also observed in an experimental investigation of channel flow by Bailey and Witte [11], who found that scaling of the PDFs could also be recovered near the wall by introducing the normalizing parameter, $\eta^*$, which depends on the wall distance and its corresponding Reynolds number.

Recently, Alhamdi and Bailey [12] examined the scaling of the PDFs in turbulent boundary layer flows with and without free-stream turbulence. They verified the suitability of using $\eta^*$ to scale the PDFs near the wall, and found that an alternative scaling parameter could be formed from $\eta_\mathcal{L} = \mathcal{L}\mathrm{Re}_\mathcal{L}^{-0.73}$, where $\mathcal{L} = K^{3/2}/\langle\varepsilon\rangle$ is a surrogate large scale which can be defined through dimensional analysis. Here, $K$ is the turbulent kinetic energy and $\langle\varepsilon\rangle$ the mean dissipation rate. It is usually assumed that $\mathcal{L} \propto L$. However, as observed by Nedić *et al.* [13], there is both wall-distance and Reynolds-number dependence in the ratio of the two scales within turbulent boundary layers. Although requiring *a priori* knowledge of $\langle\varepsilon\rangle$, the advantage of the $\eta_\mathcal{L}$ was that this scaling handled the transition between near-wall and far-wall regions much better than $\eta^*$. However, unlike in the internal wall-bounded pipe and channel flows, when a laminar free stream was present, Alhamdi and Bailey [12] reported a significant deviation in the scaling PDFs in the outer region of the turbulent boundary layer. They hypothesized that this deviation was due to statical biasing of the calculation of $\eta$ by the unsteady turbulent-nonturbulent interface between the boundary layer turbulence and laminar free stream (i.e., external intermittency) in the outer region. If not accounted for, the presence of periods of laminar flow will produce increased frequency of low measured values of $\delta_r u$ for large values of $r_1$, which will in turn increase the frequency of calculated instances where $\mathrm{Re}_\eta \sim 1$ at large $\eta$, while not actually representing an instance of dissipation at that scale. This would bias the calculated PDFs of the estimated dissipation scales towards larger values, with increasing bias towards the upper edge of the turbulent boundary layer. To support this attribution, they found a significant improvement in the scaling of the probability density functions when the free-stream conditions were turbulent. Thus, it is expected that accounting for the presence of external intermittency will improve the scaling of the PDFs, particularly when a laminar free stream is present.

It is not yet clear whether accounting for the presence of external intermittency will recover the wall-independent scaling of the PDFs observed in internal wall-bounded flows. However, if such is the case, this result could potentially be extended to other flows subject to external intermittency, such as jets and free shear layers. Thus, the objective of the present study was to revisit the data initially presented by Alhamdi and Bailey [12] using a more rigorous calculation of $\eta$ which would mitigate the influence of external intermittency.

## II. EXPERIMENT DESCRIPTION

As noted, the present study is a reexamination of data initially presented by Alhamdi and Bailey [12], specifically those for the case of a laminar free stream. Hence, only a brief description of the experiment is provided here. For a full description of this experiment and overview of the wall-normal turbulence statistics measured, the reader can refer to the earlier work.

This experiment was performed to measure the properties of a two-dimensional boundary layer developing along the flat plate when mounted in the wind tunnel and was conducted in a wind tunnel flow facility located in the Experimental Fluid Dynamics Laboratory at the University of Kentucky. This facility has a test section with a 0.61 m×0.61 m cross-section area, and a length of 1.2 m. To generate a turbulent boundary layer, a smooth flat plate with dimensions of 886 mm×608 mm was placed in the test section. To trip the boundary layer forming on the plate, it was equipped at the leading edge by 50.8 mm of a 60 grit sandpaper trip. The coordinate system origin is located at the leading edge of the plate with $x_1$ in the streamwise direction, and $x_2$ in the wall-normal direction, with $y$ also used to indicate distance from the wall, as per standard nomenclature, and $x_3$ aligned in the spanwise direction.

Measurements of the streamwise velocity profile, $U_1$, were conducted over a range of wall-normal distances, using a hot-wire probe traversed normal to the plate's surface at $x_1 = 0.76$ m. The hot-wire probe was sampled at 100 kHz and calibrated in the free-stream directly prior to, and following, each measurement run using a Pitot-static tube located in the free stream at the measurement location. The pre- and postmeasurement calibrations were used to verify that there was no voltage drift during a profile measurement.

To ensure that the smallest scales of turbulence were able to be resolved by the hot-wire probe used, the free-stream velocity was limited to $U_\infty \approx 4$ m/s. The resulting turbulent boundary layer at the measurement location had Reynolds number $\mathrm{Re}_\tau = \delta u_\tau/\nu \approx 1000$. Here, $\delta$ is the boundary layer thickness calculated at the streamwise mean velocity, $\langle U_1 \rangle = 0.99U_\infty$, found to be 82 mm. The friction velocity, $u_\tau$, was calculated by finding the value of $u_\tau$ that best scaled the measured velocity profiles in the near-wall region to the DNS data of Schlatter and Örlü [14] and was determined to be 0.19 m/s. The viscous length scale, $\nu/u_\tau$, is 79 $\mu$m and the hot-wire probe sensor length of 0.5 mm was smaller than $3\eta_K$ for the entire boundary layer thickness. Note that the flow is assumed to be stationary and ergodic, such that for the remainder of the paper $\langle\,\rangle$ is used to indicate time averaging.

## III. ANALYSIS OF THE EXTERNAL INTERMITTENCY

To account for the external intermittency in the calculation of the distribution of $\eta$ requires that we first identify instances where the transition from one state to another occurs. In other words, a turbulence detection function must be employed.

The existence of the leading and trailing edges of the turbulent bulges in the outer region of the turbulent boundary layer was first identified and studied by Corrsin and Kistler [15] using hot-wire signals. They observed that sharp changes occur during the transition from turbulent to nonturbulent motion "backs," while their counterpart "fronts" separate nonturbulent fluids from contiguous-turbulent fluids.

Detection of intermittency from a velocity time series as done by Corrsin and Kistler [15] requires application of a kinematic criterion. To identify periods of interfaces in a velocity signal, the time derivative of the velocity component [16], the derivative of the instantaneous shear stress, and the

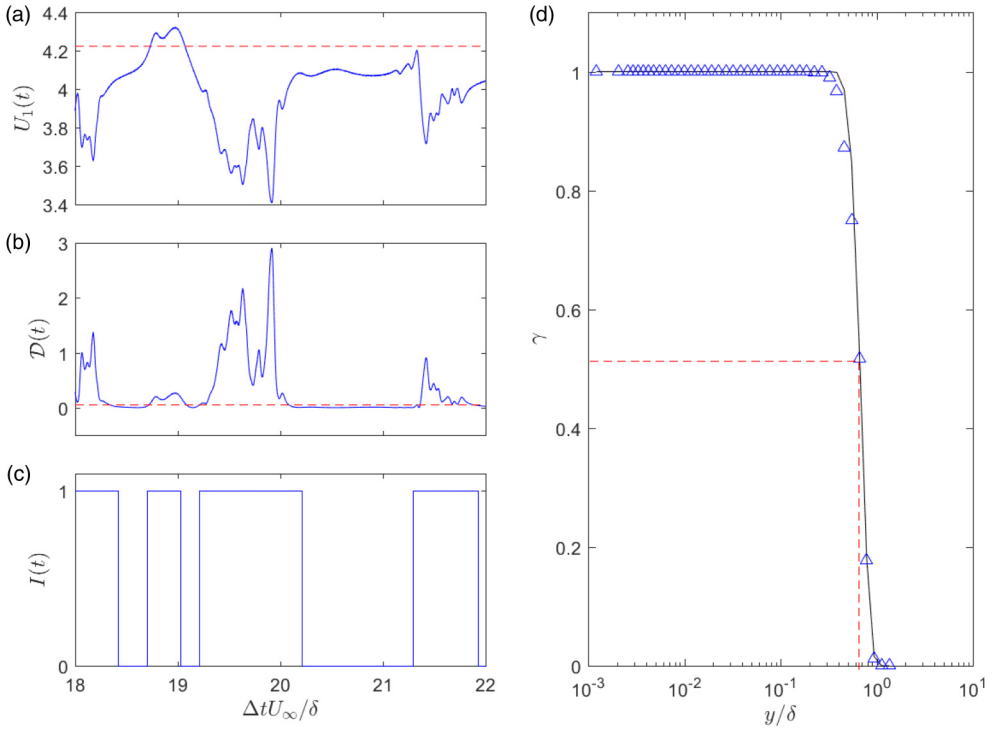


FIG. 1. (a) Portion of instantaneous streamwise velocity measured at $y/\delta = 0.66$ by the hot-wire probe, with the dashed line indicating the free-stream velocity. (b) Corresponding detector function $\mathcal{D}(t)$ with the dashed line indicating the threshold used to identify turbulent-nonturbulent zones. (c) Corresponding binary intermittency signal with $I(t) = 1$ indicating the presence of turbulence and $I(t) = 0$ indicating a nonturbulent state. (d) Profile of average intermittency function, $\gamma$. Solid line indicates Eq. (7) and dashed line indicates the wall-normal location where $\gamma = 0.5$, which occurs at $y/\delta \approx 2/3$.

magnitude of the velocity have all been previously utilized to construct different detection functions (see Hedley and Keffer [17] for a list of different turbulence detector functions utilized for hot-wire signals). Here, we have used a kinetic energy criterion suggested by Chauhan *et al.* [18] to detect turbulent-nonturbulent interfaces.

The approach is illustrated in Fig. 1. An example of the instantaneous streamwise velocity signal $U_1(t)$ is shown in Fig. 1(a), which is turbulent for some time interval and nonturbulent for the rest of the intervals. In the outer region of the turbulent boundary layer, the convection velocity of the nonturbulent flow, as it comes from the free stream, is approximately $U_\infty$ (i.e., [15,18–21]), which is denoted by the dashed line in Fig. 1(a). The detector function assumes that over the nonturbulent intervals of the signal the fluctuations $U_1 - U_\infty$ are of the order of the free-stream intensity or less. Thus, Chauhan *et al.* [18] proposed a criterion to identify these turbulent-nonturbulent interfaces by applying a threshold value on a detector function $\mathcal{D}(t) = 100 \times [1 - U_1(t)/U_\infty]^2$. When $\mathcal{D}(t)$ is less than a threshold value it is assumed to be a nonturbulent part, while it is higher than, or equals, this threshold value in the turbulent part, as shown in Fig. 1(b). In the present case, to isolate the turbulent bulges the velocity time series was low pass filtered at 25 Hz using an eighth order digital Butterworth filter (applied both forward and backward time, to eliminate any phase lag introduced into the filtered signal) before calculating $\mathcal{D}(t)$. In addition, a threshold value of $\mathcal{D}_t = 0.05$ was used [indicated by the dashed line in Fig. 1(b)], which corresponds to the 95% confidence level of a 1% standard deviation in the free-stream velocity.

Using this threshold value, the binary indicator $I(t)$ is determined where $I(t) = 0$ when $\mathcal{D}(t) < \mathcal{D}(t)_t$ and the flow is considered to be nonturbulent, and $I(t) = 1$ when $\mathcal{D}(t) > \mathcal{D}_t(t)$ and the flow is considered to be turbulent. The values of $I(t)$ for the example time series shown in Fig. 1(a) are presented in Fig. 1(c).

This calculation was conducted for all wall-normal locations to identify turbulent and nonturbulent regions at all wall-normal locations in the boundary layer. We denote the length of the turbulent intervals as $\ell_t$ and nonturbulent as $\ell_{nt}$, respectively, as illustrated in Fig. 1(c), where $\ell_t$ and $\ell_{nt}$ are found from the duration in time of each segment multiplied by the average velocity within it.

At a specific wall-normal location where the streamwise velocity is measured, the average intermittency function $\gamma$ is calculated from

$$\gamma = \frac{1}{T_s}\int_0^{T_s} I(t)dt, \tag{6}$$

in which $T_s$ is the sampling time.

In a turbulent boundary layer, the profile of $\gamma(y)$ has been found to be independent of Reynolds number [19] and can be represented with considerable accuracy by the error function as follows (see, for example, [15,17,19,22]):

$$\gamma(y) = \frac{1}{\sigma\sqrt{2\pi}}\int_y^{\infty} \exp\left[-\frac{(y-Y)^2}{2\sigma^2}\right]dy. \tag{7}$$

Here $Y$ is the mean interface position, which is the wall-normal location where $\gamma = 0.5$, and $\sigma$ is the standard deviation of the instantaneous interface position, $y$, relative to the mean location $Y$. Previous studies have found that $Y \approx 2/3\delta$ and $\sigma \approx \delta/9$ for the turbulent boundary layer [18]. Figure 1(d) shows the $\gamma$ profile measured for the turbulent boundary layer in the present study and $Y/\delta = 0.66$ was found to correspond to $\gamma = 0.52$. For comparison, the profile of $\gamma$ produced by Eq. (7) is also shown using $Y = 2/3\delta$ and $\sigma = \delta/9$. A good agreement between these two profiles of $\gamma$ was found, supporting the implementation of the $\mathcal{D}$ criterion and the selected threshold value, to identify turbulent and laminar regions within this flow.

## IV. THE EXTERNAL INTERMITTENCY EFFECT ON THE SCALING OF THE LOCAL-DISSIPATIVE SCALES

Experimental determination of $\eta$ and its PDF from hot-wire data has been previously conducted in turbulent pipe [9], channel [11], and boundary layer [12] flows. The present study essentially follows the same procedure, but had to be modified to account for the external intermittency.

Using the indicator function $I(t)$, the time series was segmented into discrete intervals, and intervals where $I(t) = 0$ were discarded. To ensure that the length of time available was suitable for determining converged PDFs, intervals where $\ell_t < 2.5\delta$ were also discarded. These remaining intervals were then analyzed as independent time series. Where intermittency was not detected, the calculation proceeded as described by Alhamdi and Bailey [12]. The calculation of the distribution of $\eta$ requires identification of instances where $\mathrm{Re}_\eta = |\delta_r u| r_1/\nu \sim 1$. To do this, $|\delta_r u|$ at each time $t$ was estimated by assuming $r_1 \approx \langle U_1\rangle \Delta t$, where $\langle U_1\rangle$ was the average velocity within the segment of time series being analyzed, and $\delta_r u \approx [u_1(t + \langle U_1\rangle \Delta t) - u_1(t)]$. For a particular discrete measurement time, $t$, $\mathrm{Re}_\eta$ was calculated over the range of $\Delta t$ values up to the length of the time series. Each instance where $\mathrm{Re}_\eta$ was between 0.5 and 2 was counted as a single occurrence of dissipation at a scale $\eta = r_1$. This process was performed for all $t$ to generate $Q(\eta)$, the count of occurrences when $0.5 < \mathrm{Re}_\eta < 2$ for each value of $\eta$.

A PDF of $\eta$ could then be found by normalizing such that $\int Q(\eta)d\eta = 1$ over the range 0 to $100\eta_{\mathcal{L}}$ where $\eta_{\mathcal{L}} = \mathcal{L}\mathrm{Re}_{\mathcal{L}}^{*-0.73}$ is also used to scale the PDFs. Note, however, that the choice in scaling parameter is not expected to impact the efficacy of the intermittency compensation, as its influence is confined to the outer layer. Scaling by $\eta_{\mathcal{L}}$ was conducted for simplicity, as it was found to be minimally

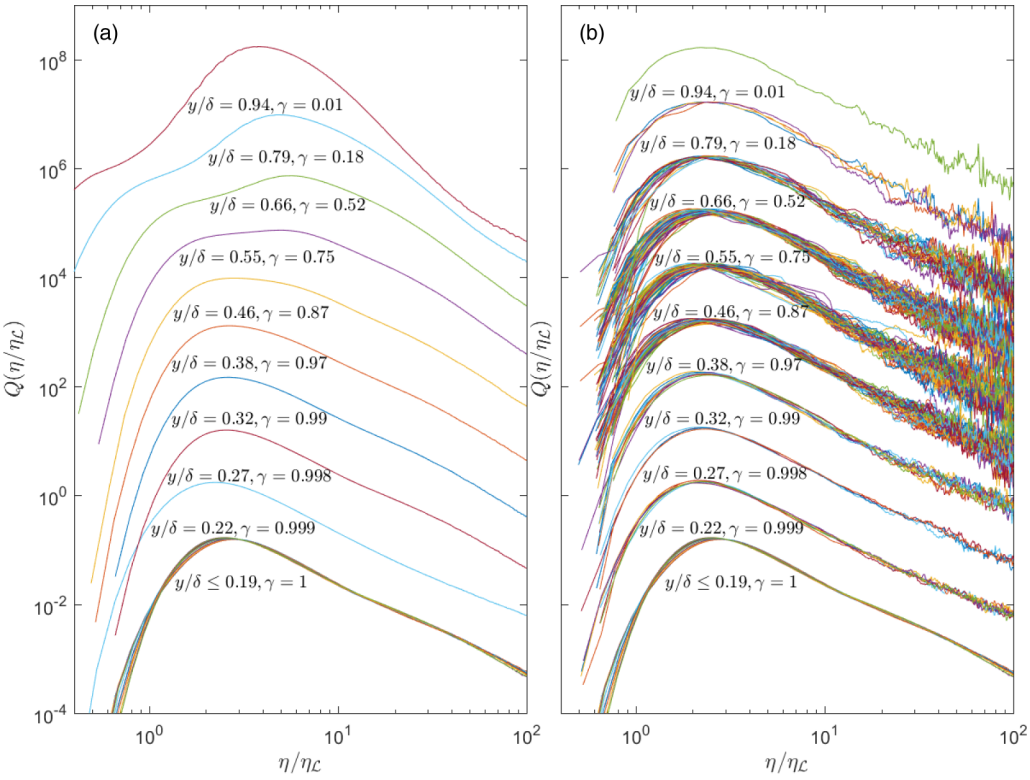


FIG. 2. Comparison between the measured PDFs of local dissipation scales when (a) treating the entire time series as turbulent and (b) accounting for the external intermittency. For cases where $\gamma < 1$ (i.e., $y/\delta > 0.19$), each wall-normal position has been shifted up by a decade for clarity.

impacted by the wall-normal location and is not bounded by ranges of validity, unlike $\eta_0$ and $\eta^*$, and thus simplifies comparison across the boundary layer [12]. To calculate $\mathcal{L} = K^{3/2}/\langle\varepsilon\rangle$, $K$ was necessarily approximated using an isotropic assumption as $1.5\langle u_1^2\rangle$ and $\langle\varepsilon\rangle$ similarly approximated as $15\nu\langle U_1\rangle^{-2}\langle(\partial u_1/\partial t)^2\rangle$. For simplicity, these quantities were calculated from the full time series, as preliminary analysis indicated that the scaling remained unchanged when $\eta_\mathcal{L}$ was calculated from only the turbulent portion of the intermittent signal.

The use of these isotropic assumptions to calculate dissipation rate was necessitated by the one-dimensional nature of the hot-wire data. However, in [11] and [12] the approach described above was compared to other methods for finding the dissipation rate from hot-wire data and the results were found to be in agreement for $y^+ > 30$, with Kolmogorov scaling of the also one-dimensional spectra supported for this range. A greater bias is likely to be introduced by the $K = 1.5\langle u_1^2\rangle$ approximation, which will bias $\mathcal{L}$ high due to anisotropy at the large scales. However, we have found the value of $\mathcal{L}\mathrm{Re}_\mathcal{L}^{-0.73}$ to change only gradually with $\mathcal{L}$ and therefore we do not expect a significant deviation in the scaling behavior to occur if mean dissipation rate and turbulent kinetic energy are calculated from the full three-component velocity vector and velocity gradient tensor.

Figure 2(a) shows the distribution of the $Q(\eta/\eta_\mathcal{L})$ at different values of $y/\delta$ without accounting for the external intermittency, in other words, by assuming the entire time series is turbulent. For cases where $\gamma$ is close to unity, the PDFs of $\eta$ collapse on one another and are consistent with previously reported distributions determined experimentally and numerically in internal wall-bounded flows [9–11], as well as other turbulent flows [8,23]. Specifically, these distributions are highly skewed and characterized by a broad tail stretching into the large scales, a peak near $\eta/\eta_\mathcal{L} \approx 2$, and a much

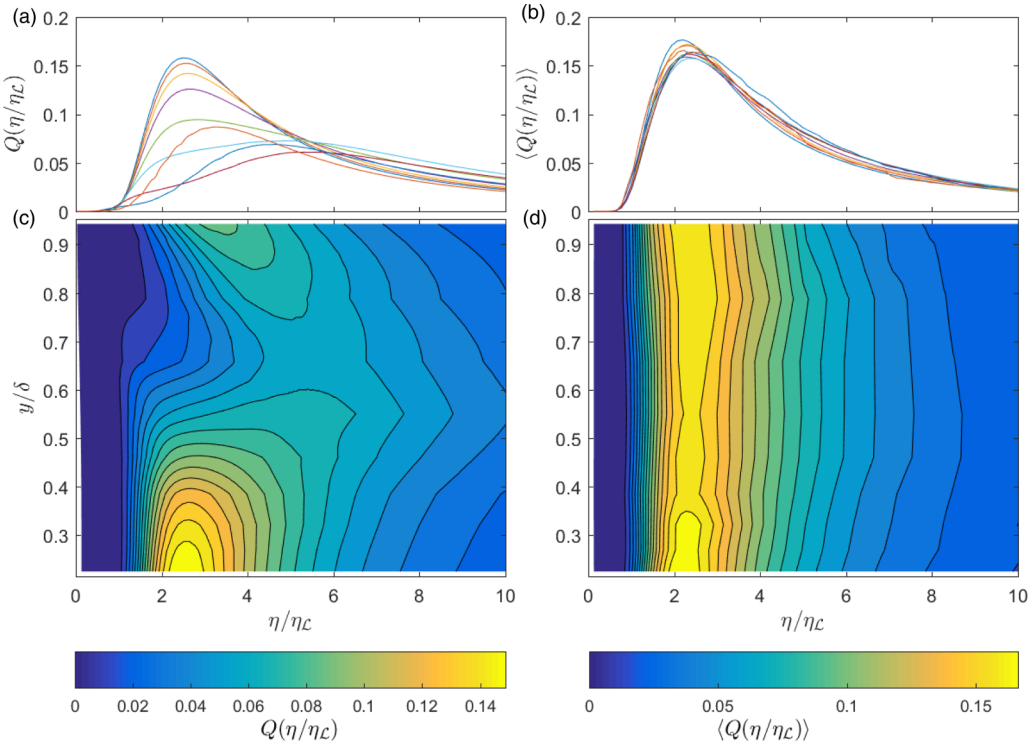


FIG. 3. PDFs of $\eta$ for cases with $\gamma < 1$ when (a) treating the entire time series as turbulent and (b) accounting for the external intermittency. For (b) the average values of the PDFs at a specific wall-normal position when the flow is intermittent are presented. Corresponding isocontours of $Q(\eta/\eta_\mathcal{L})$ as a function of $\eta/\eta_\mathcal{L}$ and $y/\delta$ are shown (c) treating the entire time series as turbulent and (d) accounting for the external intermittency.

narrower tail at small scales. However, for the cases where $\gamma < 0.9$ the PDFs become dependent on the wall-normal position, both broadening and having the maximum shift to higher values of $\eta/\eta_\mathcal{L}$.

However, when only the instances where $I(t) = 1$ and $\ell_t > 2.5\delta$ are examined, as done in Fig. 2(b), the PDFs for $\gamma < 0.9$ recover the shape of those where $\gamma > 0.9$. Note that the PDF for each segment is shown. For wall-normal locations where $\gamma$ is high, there are very few instances where the flow was identified as being laminar, and there are fewer longer segments, which improves statistical convergence of the PDFs. As $\gamma$ decreases, there are an increasing number of shorter segments which were analyzed, and there is greater scatter observed. At very low $\gamma$, the number of segments which were longer than $2.5\delta$ were fewer, limiting the number of PDFs which could be calculated at a particular wall-normal location.

To provide a more rigorous comparison of the PDFs across the different wall-normal locations, Figs. 3(a) and 3(b) show the PDF at each location in linear axes for the range of 0 to $10\eta_\mathcal{L}$. The case where the entire time series is treated as turbulent is presented in Fig. 3(a), whereas the case where only the turbulent segments of the time series are examined is presented in Fig. 3(b). For Fig. 3(b), the PDFs of each segment at a particular wall-normal distance were averaged to produce $\langle Q(\eta/\eta_\mathcal{L})\rangle$. Comparison between these figures demonstrates the improvement in scaling across the boundary layer when only the turbulent portions of the time series are considered.

The corresponding wall-distance dependence of these PDFs is demonstrated in the isocontours of $Q(\eta/\eta_\mathcal{L})$ shown in Figs. 3(c) and 3(d) as functions of $y/\delta$ and $\eta/\eta_\mathcal{L}$, again using linear scaling. Figure 3(c) shows that the greatest deviations from universal scaling occur for $y/\delta > 0.35$. In this range, the PDFs vary nonmonotonically, with the highest probabilities shifting to larger values than

those observed near the wall as $y$ increases, deviating the most at $y/\delta \approx 0.6$ and $\gamma \approx 0.5$, before shifting to smaller values near the edge of the boundary layer. Conversely, when only the turbulent segments of the time series are considered, this wall dependence is effectively removed, as shown in Fig. 3(b). Here the maximum stays constant at $\eta/\eta_{\mathcal{L}} \approx 2.2$ and only a slight broadening of the PDFs is evident at larger $\eta/\eta_{\mathcal{L}}$ for intermediate wall distances.

These results confirm the hypothesis of Alhamdi and Bailey [12] that the wall-normal dependence of the PDFs in the outer region can be attributed to bias introduced by the inclusion of periods of laminar flow in the calculation of $\eta$. More importantly, the results suggest that the boundary layer produces a universal distribution of the dissipative scales of turbulence, when turbulence is present. Given the agreement of the PDF results with those of other flows, there is consistent support for the existence of a universal distribution of these scales, one which can be determined from a single scaling parameter.

## V. CONCLUSIONS

The effects of the external intermittency on the scaling of the dissipation scale distribution were investigated in turbulent boundary layer flow at $\mathrm{Re}_\tau \approx 1000$. The analysis employed a detection function to identify the turbulent and nonturbulent regions in the outer layer where external intermittency exists. When only the turbulent portions of the time series are considered, the probability density functions of the dissipation scales from each portion of the time series collapse on each other and result in a significant improvement in the scaling of the probability density functions across the depth of the turbulent boundary layer when normalized by $\eta_{\mathcal{L}}$.

Although this observation supports the universality of the small-scale description of the turbulence for external wall-bounded flow, it should be noted that the alternative definition of the local large-scale Reynolds number, $\mathrm{Re}_{\mathcal{L}}$, presented here has only been examined in the turbulent boundary layer flow at a low Reynolds number. It is not yet clear whether the scaling parameter, $\eta_{\mathcal{L}}$, will hold for other types of shear flows or at higher Reynolds numbers. It is also not clear whether accounting for the external intermittency will generalize for other turbulent flows or at higher Reynolds numbers.

## ACKNOWLEDGMENT

This research was partially supported by the Higher Committee for Education Development (HCED) in Iraq and the University of Misan in Amarah, Iraq.

[1] F. Anselmet, Y. Gagne, E. Hopfinger, and R. Antonia, High-order velocity structure functions in turbulent shear flows, J. Fluid Mech. **140**, 63 (1984).

[2] U. Frisch, *Turbulence: The Legacy of A.N. Kolmogorov* (Cambridge University Press, Cambridge, UK, 1995).

[3] G. K. Batchelor and A. A. Townsend, The nature of turbulent motion at large wave-numbers, Proc. R. Soc. London Ser. A **199**, 238 (1949).

[4] L. Biferale, A note on the fluctuation of dissipative scale in turbulence, Phys. Fluids **20**, 031703 (2008).

[5] V. Yakhot and K. Sreenivasan, Towards a dynamical theory of multifractals in turbulence, Physica A (Amsterdam, Neth.) **343**, 147 (2004).

[6] V. Yakhot and K. R. Sreenivasan, Anomalous scaling of structure functions and dynamic constraints on turbulence simulations, J. Stat. Phys. **121**, 823 (2005).

[7] V. Yakhot, Probability densities in strong turbulence, Physica D **215**, 166 (2006).

[8] J. Schumacher, Sub-Kolmogorov-scale fluctuations in fluid turbulence, Europhys. Lett. **80**, 54001 (2007).

[9] S. C. C. Bailey, M. Hultmark, J. Schumacher, V. Yakhot, and A. J. Smits, Measurements of the Dissipation Scales in Turbulent Pipe Flow, Phys. Rev. Lett. **103**, 014502 (2009).

[10] P. Hamlington, D. Krasnov, T. Boeck, and J. Schumacher, Local dissipation scales and energy dissipation-rate moments in channel flow, J. Fluid Mech. **701**, 419 (2012).
[11] S. C. C. Bailey and B. M. Witte, On the universality of local dissipation scales in turbulent channel flow, J. Fluid Mech. **786**, 234 (2016).
[12] S. F. H. Alhamdi and S. C. C. Bailey, Universality of local dissipation scales in turbulent boundary layer flows with and without free-stream turbulence, Phys. Fluids **29**, 115103 (2017).
[13] J. Nedić, S. Tavoularis, and I. Marusic, Dissipation scaling in constant-pressure turbulent boundary layers, Phys. Rev. Fluids **2**, 032601 (2017).
[14] P. Schlatter and R. Örlü, Assessment of direct numerical simulation data of turbulent boundary layers, J. Fluid Mech. **659**, 116 (2010).
[15] S. Corrsin and A. L. Kistler, The freestream boundaries of turbulent flows, NACA-TN-3133, 1954, https://ntrs.nasa.gov/archive/nasa/casi.ntrs.nasa.gov/19930092246.pdf.
[16] Y. Tsuji, K. Honda, I. Nakamura, and S. Sato, Is intermittent motion of outer flow in the turbulent boundary layer deterministic chaos? Phys. Fluids A **3**, 1941 (1991).
[17] T. B. Hedley and J. F. Keffer, Some turbulent/non-turbulent properties of the outer intermittent region of a boundary layer, J. Fluid Mech. **64**, 645 (1974).
[18] K. Chauhan, J. Philip, C. M. de Silva, N. Hutchins, and I. Marusic, The turbulent/non-turbulent interface and entrainment in a boundary layer, J. Fluid Mech. **742**, 119 (2014).
[19] H. Fiedler and M. Head, Intermittency measurements in the turbulent boundary layer, J. Fluid Mech. **25**, 719 (1966).
[20] J. Jiménez, S. Hoyas, M. P. Simens, and Y. Mizuno, Turbulent boundary layers and channels at moderate Reynolds numbers, J. Fluid Mech. **657**, 335 (2010).
[21] L. S. Kovasznay, V. Kibens, and R. F. Blackwelder, Large-scale motion in the intermittent region of a turbulent boundary layer, J. Fluid Mech. **41**, 283 (1970).
[22] C.-H. P. Chen and R. F. Blackwelder, Large-scale motion in a turbulent boundary layer: A study using temperature contamination, J. Fluid Mech. **89**, 1 (1978).
[23] J. Schumacher, J. Scheel, D. Krasnov, D. Donzis, V. Yakhot, and K. R. Sreenivasan, Small-scale universality in fluid turbulence, Proc Natl. Acad. Sci. USA **111**, 10961 (2014).